

Mechanism of mechanical relaxation associated with precipitates

This article has been downloaded from IOPscience. Please scroll down to see the full text article.

1989 J. Phys.: Condens. Matter 1 10039

(<http://iopscience.iop.org/0953-8984/1/50/006>)

View [the table of contents for this issue](#), or go to the [journal homepage](#) for more

Download details:

IP Address: 171.66.16.96

The article was downloaded on 10/05/2010 at 21:18

Please note that [terms and conditions apply](#).

Mechanism of mechanical relaxation associated with precipitates

Yening Wang, Min Gu and Linhai Sun

Laboratory of Solid States Microstructure, Nanjing University, Nanjing, People's Republic of China

Received 9 February 1989

Abstract. The thermal activated relaxation connected with precipitates in a number of alloys always exhibits a broad and asymmetric peak in T^{-1} plots, which is very different from the Debye-type relaxation peak. Because solute clustering is present around the precipitates, a strong correlation should exist between the motions of solute atoms. Ngai's correlated-state model is used to simulate the relaxation spectrum. The calculation results not only correlate quite well with the experimental data on the Al–Ag, Ti–H and Ta–H systems but also have profound implications on the mechanism of the internal friction peak.

1. Introduction

There are two types of internal friction associated with precipitation in alloys. One occurs during precipitation, and its peak height decreases with increasing measurement frequency f and decreases with decreasing cooling (or heating) rate. This is not a relaxation peak and is referred to as a precipitation peak [1]. The other type is a relaxation peak closely related to the precipitates. Only the second case will be studied in this paper.

For Al–Ag alloys a peak near 140 °C (0.25 Hz) [2] is initially due to the presence of clusters of solute atoms and later to the plate-like transition γ' precipitates (HCP). The peak at about 200 K in the Ta–H system [3] has been attributed to the motion of hydrogen in the β_2 -phase precipitates (BCT). The peak P_2 (209 K) in the Ti–H system [4] is considered to be associated with hydride precipitates (FCT) and is attributed to the motion of hydrogen atoms. This thermally activated relaxation connected with precipitates in spite of the quite different structures in various alloys always exhibits a broad and asymmetric peak in T^{-1} plots, which is very different from the Debye-type relaxation peak and is similar to the relaxation peaks in amorphous dielectrics. Ngai's [5] correlated-state model has been used to simulate the non-Debye relaxation spectrum in amorphous materials, giving satisfactory results. In the case of precipitates in crystalline materials the solute clusters are found to be present around [6, 7] or within [3] the precipitates and, even at local equilibrium under applied stress, there can be a change leading to a limited resolution in some areas of the precipitate and further precipitation in others, which is accompanied by a change in the arrangement of solute atoms from order to disorder or vice versa. So we speculate that the peak must be ascribed to correlated motion of the atoms in a solute cluster instead of the uncorrelated motion of atoms as

implied in the papers published so far, and thus we try to apply Ngai's theory to the relaxation due to precipitates. This is the first attempt to do this for crystalline solids. According to expectations, it enjoys the same degree of success in this case as it does for relaxation in amorphous materials.

2. Non-Debye relaxation theory based on the correlated-states model

It is well known that Debye relaxation is a pure exponential decay:

$$\varphi(t) = \varphi_0 \exp(-t/\tau_0) \quad (1)$$

which gives a frequency-dependent dynamic response function

$$\chi(\omega) = \chi(0)/(1 + i\omega\tau_0)$$

where τ_0 is known as the Debye relaxation time and the energy loss $\text{Im}[\chi(\omega)]$ is a symmetric Debye peak. However, experimental data on relaxation in many types of condensed matter especially in glass-like or disordered system are quite generally found to exhibit slower than exponential decay for long times in the fractional exponential decay form

$$\varphi(t) = \varphi_0 \exp[-(t/\tau_p)^{1-n}] \quad 0 \leq n < 1 \quad (2)$$

and the loss peak becomes asymmetric and broader than Debye peak. Usually, the distribution $g(\tau)$ of relaxation times is introduced into the response function

$$\chi(\omega) = \int_0^\infty \frac{g(\tau)}{1 + i\omega\tau} d\tau \quad (3)$$

but this approach only reduces the problem to another physically unverifiable quantity $g(\tau)$.

Ngai proposed a correlated-state model [5]. In disordered systems, many correlated energy states always exist with small level spacings and low-energy excitation and de-excitation. As a result, the transition rate τ_0^{-1} is modified by the infrared divergent excitations and de-excitations of correlated states to be time dependent, i.e. $[\tau(t)]^{-1}$ given by

$$[\tau(t)]^{-1} = \tau_0^{-1} \exp(-n\gamma)(E_c t)^{-n} \quad 0 \leq n < 1 \quad E_c t \gg 1 \quad (4)$$

where n is the infrared divergent index or correlation index, $\gamma = 0.577$ and E_c is the upper 'cut-off' of the correlated-state excitation energy, which can be considered as the energy above which the density of correlated-state excitation is no longer linear in E (this very linearity leads to the infrared divergent response). $\tau_0 = \tau_\infty \exp(E_a/kT)$, where τ_∞ and E_a determine the microscopic dynamics and energy of the fundamental process

in the absence of strong correlations ($n = 0$). The relaxation function (2) may be obtained when equation (4) is substituted into rate equation, where τ_p is related to τ_0 by

$$\tau_p = [(1 - n) \exp(n\gamma) E_c^n \tau_0]^{1/(1-n)}. \quad (5)$$

Let E_a^* denote the apparent activation energy; we then have

$$\tau_p = \tau_\infty^* \exp(E_a^*/kT) \quad (6)$$

$$E_a^* = E_a/(1 - n). \quad (7)$$

Based on the fluctuation dissipation theory, the energy loss Q^{-1} can be written as

$$Q^{-1} = \pi \Delta \omega \tau_p Q_\alpha(\omega \tau_p) = \pi \Delta Z Q_\alpha(Z) \quad (8)$$

where Δ is the relaxation strength; $Z = \omega \tau_p$; $Q_\alpha(Z)$ is the Lévy function given by

$$Q_\alpha(Z) = \frac{1}{2\pi} \int_{-\infty}^{\infty} \exp(-i Z u - u^\alpha) du \quad (9)$$

with $u = t/\tau_p$ and $\alpha = 1 - n$. Since $Z = \omega \tau_p = \omega \tau_\infty^* \exp(E_a^*/kT)$ is a function of frequency as well as temperature T , both the frequency spectrum and the temperature spectrum may be calculated using the Lévy function. Exhaustive comparisons with experimental data for various relaxation phenomena in many types of amorphous condensed matter have been made. The fractional exponential decay property of relaxation in (2) and, for the same n , the fact that τ_p and τ_0 are related by (5) have been widely verified [8–12]. The values of n may not be the same for different primary relaxation species (i.e. ionic, molecular, macromolecular, electronic, etc) and for different materials (glasses, amorphous polymers, ionic conductors, etc).

Subsequently a description was provided [13, 14] of the physical origin of the universality relations (2) and (5) in terms of the concept of an irregular quantum system which is described as the level system (LS). The system undergoing relaxation is referred to as a primary species (PS) which is assumed to be in contact with the LS as well as with a very large heat sink. The energy spectrum of the irregular quantum system plays an important role in the non-exponential relaxation. Any large quantum system whose classical motion is irregular but the quantum level spacing is fairly regularly distributed, i.e. the probability density $N(E)$ for the level spacing E between two neighbouring levels has a linear relation up to an upper cut-off spacing energy E_c , was considered in [13, 14]. The coupling of the PS to the LS structure generated LS excitation and then modified the time-independent transition rate τ_0^{-1} to a time-dependent transition rate $[\tau(t)]^{-1}$ of the form (4).

The effect of the PS–LS interaction on the transition rate may be understood easily as follows. After the PS is itself driven away from equilibrium by an external field, its interaction with the LS excitation drives the latter away from equilibrium. The PS–LS interaction reduces the entropy of the LS excitation, because the LS excitation has a maximum entropy at equilibrium. The relaxation rate is modified by operating in an environment with decreased entropy. At a fixed temperature T , the entropy decrease $\Delta S_{LS}(t)$ in the environment is only the time-dependent contribution to the free energy controlling the behaviour of the relaxation rate. By analogy to the reaction rate theory, the transition rate may be written as

$$[\tau(t)]^{-1} = \tau_0^{-1} \exp[-\Delta S_{LS}(t)/k]. \quad (10)$$

The calculation of the entropy evolution of the LS excitations shows that ΔS_{LS} has a logarithmic time dependence that yields the same form as (4).

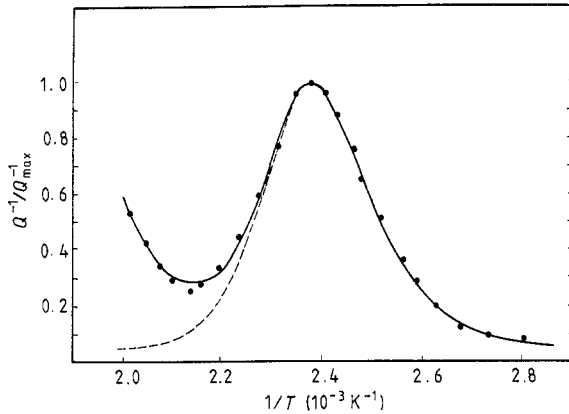


Figure 1. Normalised internal friction peak of Al-20.1 wt% Ag alloy ($f = 1$ Hz): ●, experimental data taken from a specimen annealed for a long time [2]; —, theoretical curve with the exponential background subtracted in the simulation process; ---, theoretical curve without the exponential background subtracted in the simulation process.

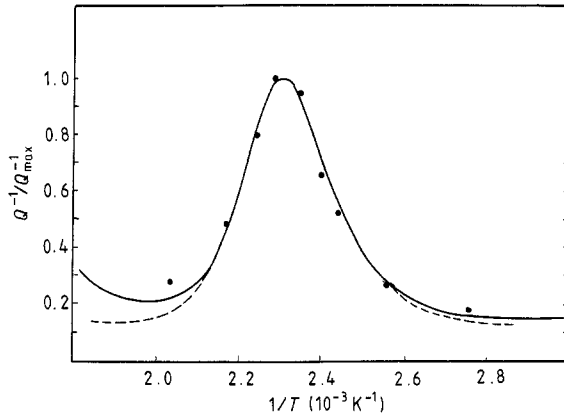


Figure 2. Normalised internal friction peak of Al-20 wt% Ag alloy ($f = 0.25$ Hz): ●, experimental data taken from a specimen annealed at 520 °C for 3 h [7]; —, theoretical curve with the exponential background subtracted in the simulation process; ---, theoretical curve without the exponential background subtracted in the simulation process.

In the case of internal friction due to precipitates, the solute cluster is the LS which has many energy levels with a small level spacing, and each solute atom in the cluster plays the role of the PS.

3. Results of calculation and comparison with experimental data

Quite a few internal friction peaks related to precipitates in several alloys have been calculated. Only those peaks with the lowest background on both the high- and the low-temperature sides were taken into account, so that the error due to the deduction of the background may be neglected. The results for five kinds of alloy are shown in figures 1–5: Al-20.1 wt% Ag [2] in figure 1; Al-20 wt% Ag [7] in figure 2; Al-30 wt% Ag [7] in figure 3; Ti-5 at.% H [4] in figure 4; Ta-5 at.% H [3] in figure 5. The model quantities E_a^* and n in the Lévy function were adjusted to give the best fit with the position and shape of each internal friction peak. The calculated curves with the background subtracted shown by the full curves in the figures are in quite good agreement with the internal friction data.

The calculated values of the apparent activation energy E_a^* (which governs the lateral shift of the internal friction peak along the temperature axis as the frequency is varied),

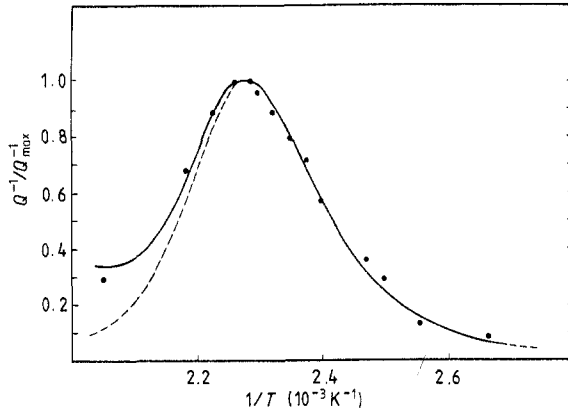


Figure 3. Normalised internal friction peak of Al-30 wt% Ag alloy ($f = 0.25$ Hz): ●, experimental data taken from a specimen annealed at 520 °C for 3 h [7]; —, theoretical curve with the exponential background subtracted in the simulation process; ---, theoretical curve without the exponential background subtracted in the simulation process.

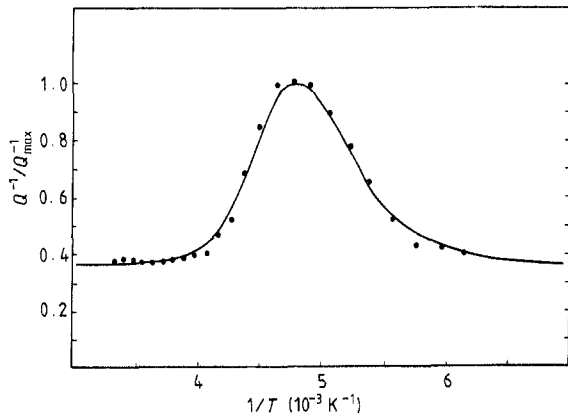


Figure 4. Normalised internal friction spectra of Ti-5.4 at.% H measured at $f = 1.5$ Hz: ●, experimental data [4]; —, theoretical curve with the background subtracted in the simulation process.

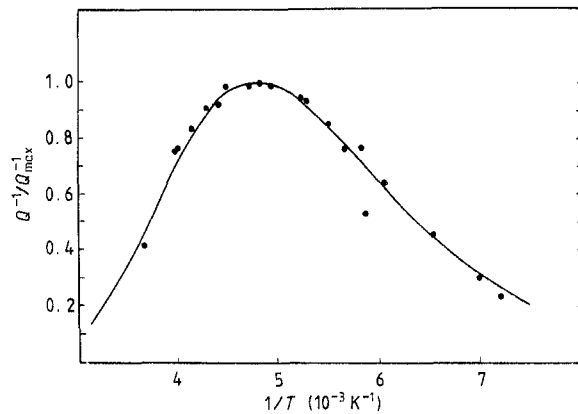


Figure 5. Normalised internal friction spectra of Ta-5 at.% H ($f = 26$ kHz): ●, experimental data measured on heating after several thermal cycles so that any kinetic effect due to precipitation is avoided and the peak height reaches saturation [3]; —, theoretical curve.

the correlation index n and the true activation energy E_a (which is related to E_a^* by $E_a^* = E_a/(1 - n)$) are shown in table 1. For comparison, the experimental activation energy values E_a^+ (obs.) are also included; they are nearly the same as E_a^* (calc.). It is

Table 1. The observed apparent activation energy $E_a^*(\text{obs.})$, the calculated apparent activation energy $E_a^*(\text{calc.})$, the true activation energy E_a and the correlation index n .

Alloy	Structure of alloy	Structure of precipitate	$E_a^*(\text{obs.})$ (eV)	$E_a^*(\text{calc.})$ (eV)	E_a (eV)	n
Al-30 wt% Ag	FCC	HCP	1.2 ± 0.1	1.3	0.91	0.3
Al-20 wt% Ag	FCC	HCP	1.2 ± 0.1	1.3	0.91	0.3
Al-20.1 wt% Ag	FCC	HCP	1.09 ± 0.02	1.3	0.91	0.3
Ta-5 at.% H	BCC	BCT	0.38 ± 0.05	0.40	0.10	0.75
Ti-5.4 at.% H	HCP	FCT	0.47 ± 0.01	0.47	0.25	0.44

surprising to note that all the internal friction peaks for Al–Ag alloys, even with different compositions and from different workers, have nearly the same values of E_a^* , E_a and n .

In addition, the fact that the values of the true activation energy E_a are lower than those for diffusion in solid solution is consistent with the presence of distortion on the interfaces and disordered solute clusters.

4. Discussion

The predictions of the theory not only correlate quite well with the experimental data but also have profound implications on the mechanism of the internal friction peak. Various mechanisms have been proposed so far for the static internal friction peak associated with precipitates as classified below [1, 15]:

- (i) the relaxation of dislocations surrounding the precipitates (with or without solute atom);
- (ii) the stress-induced change in the particle shape (i.e. precipitation and dissolution) for which the rate-limiting process is atom migration around the matrix–precipitate interface;
- (iii) hydrides themselves, and diffusion of hydrogen in hydrides;
- (iv) the relaxation of atom groupings within the individual clusters.

According to our point of view, the correlated motion instead of uncorrelated motion of the atoms in a solute cluster is responsible for the relaxation. Firstly, mechanism (i) based on dislocation relaxation without a solute atom must be ruled out. If a solute atmosphere occurs around the dislocation, the correlated motion of solute atoms is possible, but it should be further confirmed by comparison with the Snoek–Koster peak in BCC alloys. The solute clusters may also exist near the interface between precipitates and matrix (mechanism (ii)) and even within hydrides (mechanism (iii)) as suggested in [3] in the light of neutron scattering experiments; so a strong correlation should exist between the motions of solute atoms, resulting in the successful application of the correlated-state model.

In this model, it is easy to understand why the internal friction peaks due to the Ag clusters (mechanism (iv)) and due to γ' precipitates (mechanism (ii)) in Al–Ag alloys have the same peak temperature, which has never been explained before.

For the Ta–H system (see table 1), it is puzzling why $E_a^*(\text{obs.})$ ($=0.38$ eV) in the β_2 -phase is much larger than the activation energy (0.12 eV) of hydrogen in α -Ta

phase. However, it is reasonable if we take into account the true activation energy value E_a ($=0.10$ eV), which is comparable with 0.12 eV.

Calculations for the K \ddot{o} ster peak induced by the Cottrell atmosphere around dislocation and other peaks will be carried out and therefore some new information on the mechanism will be obtained.

5. Conclusions

(i) The internal friction peak associated with precipitates in alloys always exhibits a non-Debye relaxation character with a broad and asymmetric peak in T^{-1} plots.

(ii) Ngai's correlated-state model is used to simulate the peak due to precipitates. The calculation results coincide with the experimental data on Al–Ag, Ti–H and Ta–H systems quite well.

(iii) The mechanism of the precipitation peak is considered to be related to the correlated motion of atoms in solute clusters instead of to uncorrelated solute atoms as implied in the papers published so far. The clusters may exist on the interface between precipitates and the matrix under the action of stress, on the dislocations around precipitates and in some hydrides.

References

- [1] Koiwa M and Yoshimari O 1985 *J. Physique Coll.* **46** C10–99
- [2] Damask A C and Nowick A S 1955 *J. Appl. Phys.* **26** 1165
- [3] Cannelli G and Mazzolai F M 1969 *Nuovo Cimento B* **64** 171
- [4] Numakura H and Koiwa M 1985 *Trans. Japan. Inst. Metall.* **26** 653
- [5] Ngai K L 1979 *Phys. Rev. B* **20** 2435; 1979 *Comments Solid State* **9** 127
- [6] Entwistle K M 1953–4 *J. Inst. Met.* **82** 249; 1956–7, *J. Inst. Met.* **85** 425
- [7] Schoeck G and Bisogri E 1969 *Phys. Status Solidi* **32** 31
- [8] Fan Xiqing, Wang Guoliang, Jiang Wangyi, Dai Peiying and Liu Fusui 1985 *Acta Phys. Sin.* **34** 1270
- [9] Fan Xiqing, Wang Guoliang and Liu Fusui 1986 *Acta Phys. Sini.* **35** 896
- [10] Gao Guoru and Ngai K L 1981 *Ke-Xue Tong-Bao* **26** 844
- [11] Wang Yangpu and Gao Guoru 1985 *J. Physique Coll.* **46** C10 465
- [12] Wang Yangpu and Jin Qishu 1988 *Acta Phys. Sin.* **37** 1083
- [13] Rajagopal A K and Wiegel F W 1984 *Physica A* **127** 218
- [14] Rajagopal A K, Teitler S and Ngai K L 1984 *J. Phys. C: Solid State Phys.* **17** 6611
- [15] Nowick A S and Berry B S 1972 *Anelastic Relaxation in Crystalline Solids* (New York: Academic) p 490